Available online at www.sciencedirect.com
SCIENCE DIRECT®
Applied Numerical Mathematics 52 (2005) 381–400
APPLIED NUMERICAL MATHEMATICS
www.elsevier.com/locate/apnum

Quadratic optimization in the problems of active control of sound ☆

J. Lončarić [a,1], S.V. Tsynkov [b,*]

[a] *Los Alamos National Laboratory, MS-D432, P.O. Box 1663, Los Alamos, NM 87545, USA*
[b] *Department of Mathematics and Center for Research in Scientific Computation (CRSC), North Carolina State University, Box 8205, Raleigh, NC 27695, USA*

Abstract

We analyze the problem of suppressing the unwanted component of a time-harmonic acoustic field (noise) on a predetermined region of interest. The suppression is rendered by active means, i.e., by introducing the additional acoustic sources called controls that generate the appropriate anti-sound. Previously, we have obtained general solutions for active controls in both continuous and discrete formulation of the problem. We have also obtained optimal solutions that minimize the overall absolute acoustic source strength of active control sources, which is equivalent to minimization in the sense of L_1.

By contrast, in the current paper we formulate and study optimization problems that involve quadratic functions of merit. Specifically, we minimize the L_2 norm of the control sources, and we consider both the unconstrained and constrained minimization. The unconstrained L_2 minimization is an easy problem to address numerically. On the other hand, the constrained approach allows one to analyze sophisticated geometries. In a special case, we can compare our finite-difference optimal solutions to the continuous optimal solutions obtained previously using a semi-analytic technique. We also show that the optima obtained in the sense of L_2 differ drastically from those obtained in the sense of L_1.

☆ This research was supported by the National Aeronautics and Space Administration under NASA Contract No. NAS1-97046, and by the Langley Research Center Creativity and Innovation Program (C&I), while both authors were in residence at ICASE, NASA Langley Research Center, Hampton, VA 23681-2199, USA.

* Corresponding author.
E-mail addresses: josip@lanl.gov (J. Lončarić), tsynkov@math.ncsu.edu (S.V. Tsynkov).
URL: http://www.math.ncsu.edu/~stsynkov.

[1] The author was a Research Fellow at ICASE when this paper was written.

0168-9274/$30.00 © 2004 IMACS. Published by Elsevier B.V. All rights reserved.
doi:10.1016/j.apnum.2004.08.041

Keywords: Noise cancellation; Active control sources; Volumetric and surface controls; General solution; Monopoles and dipoles; Radiation of waves; Complex-valued quantities; L_2-minimization; Overdetermined systems; Least squares; Unconstrained minimization; Constrained minimization

1. Introduction

In the simplest possible formulation, the problem of active control of sound is posed as follows. Let $\Omega \subset \mathbb{R}^n$ be a given domain (bounded or unbounded), and Γ be its boundary: $\Gamma = \partial\Omega$, where the dimension of the space n is either 2 or 3. Both on $\overline{\Omega} = \Omega \cup \Gamma$ and on its complement $\Omega_1 = \mathbb{R}^n \setminus \overline{\Omega}$ we consider the time-harmonic acoustic field $u = u(\mathbf{x})$, $\mathbf{x} \in \mathbb{R}^n$, governed by the nonhomogeneous Helmholtz equation:

$$\mathbf{L}u \equiv \Delta u + k^2 u = f. \tag{1}$$

Eq. (1) is subject to the Sommerfeld radiation boundary conditions:

$$u(\mathbf{x}) = \mathrm{O}\big(|\mathbf{x}|^{(1-n)/2}\big), \qquad \frac{\partial u(\mathbf{x})}{\partial |\mathbf{x}|} + iku(\mathbf{x}) = \mathrm{o}\big(|\mathbf{x}|^{(1-n)/2}\big), \quad \text{as } |x| \to \infty, \tag{2}$$

which specify the direction of wave propagation at infinity, and distinguish between the incoming and outgoing waves by prescribing the outgoing direction only; they guarantee the unique solvability of the Helmholtz equation (1) for any compactly supported right-hand side $f = f(\mathbf{x})$. Note that as we are dealing with the traveling waves (radiation of sound toward infinity), all the resulting solutions necessarily have to be complex-valued, otherwise it is impossible to account for the key phenomenon of variation of phase with the change of spatial location. We should also mention that the choice of the sign "+" or "−" in the second expression of (2) that actually selects the direction of propagation is basically a matter of convention; it only has to correlate with the definition of the direct/inverse Fourier transform (again, "+" or "−" in the exponent) adopted for transforming the unsteady wave equation into the Helmholtz equation (1). In the literature, the "−" sign is often used for the Sommerfeld radiation boundary conditions; we would rather keep the sign "+" in formula (2) to make it consistent with our previous publications on the subject of active noise control [6,14,4,5].

The source terms $f = f(\mathbf{x})$ in Eq. (1) can be located on both Ω and its complement $\Omega_1 = \mathbb{R}^n \setminus \overline{\Omega}$; to emphasize the distinction, we denote

$$f = f^+ + f^-, \quad \operatorname{supp} f^+ \subset \Omega, \ \operatorname{supp} f^- \subset \Omega_1. \tag{3}$$

Accordingly, the overall acoustic field $u = u(\mathbf{x})$ can be represented as a sum of the two components:

$$u = u^+ + u^-, \tag{4}$$

where u^+ is driven by the interior sources f^+, and u^- is driven by the exterior sources f^- w.r.t. Ω:

$$\mathbf{L}u^+ = f^+, \tag{5a}$$

$$\mathbf{L}u^- = f^-. \tag{5b}$$

Note, both $u^+ = u^+(\mathbf{x})$ and $u^- = u^-(\mathbf{x})$ are defined on the entire $\mathbb{R}^n$, the superscripts "+" and "−" refer to the sources that drive each of the field components rather than to the domains of these components. The setup described above is schematically shown in Fig. 1 for the case of a bounded domain Ω.

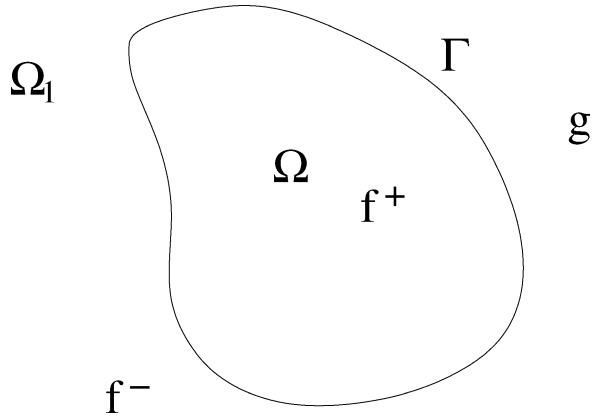

Fig. 1. Geometric setup.

Hereafter, we will call the component u^+ of (4), (5a) *sound*, or "friendly" part of the total acoustic field; the component u^- of (4), (5b) will accordingly be called *noise*, or "adverse" part of the total acoustic field. In the formulation that we are presenting, Ω will be a predetermined region of space to be protected from noise. This means that we would like to eliminate the noise component of $u(\mathbf{x})$ inside Ω, while leaving the sound component there unaltered. In the mathematical framework that we have adopted, the component u^- of the total acoustic field, i.e., the response to the adverse sources f^- (see (3)–(5)), will have to be canceled out on Ω, whereas the component u^+, i.e., the response to the friendly sources f^+, will have to be left unaffected on Ω. A physically more involved but conceptually easy to understand example that can be given to illustrate the foregoing idea, is that inside the passenger compartment of an aircraft we would like to eliminate the noise coming from the propulsion system located outside the fuselage, while not interfering with the ability of the passengers to listen to the inflight entertainment programs or simply converse.

The concept of *active noise control* implies that the component u^- is to be suppressed on Ω by introducing additional sources of sound $g = g(\mathbf{x})$ exterior with respect to Ω, $\operatorname{supp} g \subset \overline{\Omega}_1$, so that the total acoustic field $\tilde{u} = \tilde{u}(\mathbf{x})$ be now governed by the equation (cf. formulae (1), (3)):

$$\mathbf{L}\tilde{u} = f^+ + f^- + g, \tag{6}$$

and coincide with only the friendly component u^+ on the domain Ω:

$$\tilde{u}|_{\mathbf{x}\in\Omega} = u^+|_{\mathbf{x}\in\Omega}. \tag{7}$$

The new sources $g = g(\mathbf{x})$ of (6), see Fig. 1, will hereafter be referred to as the *control sources* or simply *controls.* An obvious solution for these control sources is $g = -f^-$. This solution, however, is clearly sub-optimal because on one hand, it requires an explicit and detailed knowledge of the structure and location of the sources f^-, which is, in fact, superfluous, see [6]. On the other hand, its implementation in many cases, like in the previously mentioned example with an airplane, may not be feasible. Fortunately, there are other solutions of the foregoing noise control problem (see Section 2, as well as our previous work [6,4,5] for details), and some of them may be preferable from both the theoretical and practical standpoint.

To conclude the introduction, let us only mention that the area of active control of sound has a rich history of development, both as a chapter of theoretical acoustics, and in the perspective of many different

applications. It is impossible to adequately overview this extensive area in the framework of a focused research publication. As such, we simply refer the reader to the monographs [8,2,1] that, among other things, contain a detailed survey of the literature. Potential applications for the active techniques of noise control range from the aircraft industry to manufacturing industry to ground and air transportation to the military to consumer products and other fields, including even such highly specialized and narrow areas as acoustic measurements in the wind tunnels. It is generally known that active techniques are more efficient for lower frequencies, and they are usually expected to complement passive strategies (sound insulation, barriers, etc.) that are more efficient for higher frequencies, because the rate of sound dissipation due to the viscosity of the medium and heat transfer is proportional to the square of the frequency [3].

Let us also note that in the current paper we focus on the case of the standard constant-coefficient Helmholtz equation (1), which governs the acoustic field throughout the entire space $\mathbb{R}^n$. This allows us to make the forthcoming analysis most straightforward. However, one can also consider other, more complex, cases that involve variable coefficients, different types of far-field behavior, discontinuities in the material properties, and maybe even nonlinearities in the governing equations over some regions. Approaches to obtaining solutions for active controls in these cases are based on the theory of generalized Calderon's potentials and boundary projections, and can be found in our previous paper [6] and in the monograph by Ryaben'kii [12, Part VIII].

The material in the rest of the paper is organized as follows. In Section 2, we introduce and discuss general solutions for controls in the continuous and discrete framework. Section 3 is devoted to the formulation and solution of the quadratic optimization problems for the control sources (unconstrained and constrained L_2 optimization). For reference purposes we also briefly mention our previous results on the optimization in the sense of L_1. Finally, Section 4 summarizes our current findings and also contains some general discussion.

2. General solutions for control sources

2.1. Continuous formulation of the problem

A general solution for the volumetric continuous control sources $g = g(\mathbf{x})$ is given by the following formula ($\Omega_1 = \mathbb{R}^n \setminus \overline{\Omega}$):

$$g(\mathbf{x}) = -\mathbf{L}w|_{\mathbf{x}\in\Omega_1}, \tag{8}$$

where $w = w(\mathbf{x})$, $\mathbf{x} \in \Omega_1$, is a special auxiliary function-parameter that parameterizes the family of controls (8). The function $w(\mathbf{x})$ must satisfy the Sommerfeld boundary conditions (2) at infinity, and at the interface Γ, the function w and its normal derivative have to coincide with the corresponding quantities that pertain to the total acoustic field u given by formula (4):

$$w|_\Gamma = u|_\Gamma, \qquad \frac{\partial w}{\partial \mathbf{n}}\Big|_\Gamma = \frac{\partial u}{\partial \mathbf{n}}\Big|_\Gamma. \tag{9}$$

Other than that, the function $w(\mathbf{x})$ used in (8) is arbitrary, and consequently formula (8) defines a large family of control sources, which provides ample room for optimization. The justification for formula (8) as the general solution for controls can be found in [6]. In [4], we also emphasize that the controls

$$g(\mathbf{x}) = \int g(\mathbf{y})\delta(\mathbf{x}-\mathbf{y})\,\mathrm{d}\mathbf{y} = g * \delta,$$

given by (8) are actually *volumetric control sources of the monopole type* with regular (locally absolutely integrable) density $g \in L_1^{(\mathrm{loc})}(\mathbb{R}^n)$.

The control sources (8) possess several important properties that are discussed in detail in [6]. Here we only summarize that they do not require any knowledge of the actual exterior sources of noise f^- and are built based solely on the measurable quantities $u|_\Gamma$ and $\frac{\partial u}{\partial \mathbf{n}}|_\Gamma$. Besides, while these measurable input data pertain to the overall acoustic field, the controls appear insensitive to the interior sound u^+ and specifically target the exterior noise u^- on Ω.

Along with the volumetric controls (8), one can also consider *surface controls*, i.e., the control sources that are concentrated only on the interface Γ. A general solution for the surface controls is given by

$$g^{(\mathrm{surf})} = -\left[\frac{\partial w}{\partial \mathbf{n}} - \frac{\partial u}{\partial \mathbf{n}}\right]_\Gamma \delta(\Gamma) - \frac{\partial}{\partial \mathbf{n}}\big([w-u]_\Gamma \delta(\Gamma)\big), \tag{10}$$

where the auxiliary function-parameter $w = w(\mathbf{x})$ now has to satisfy the Helmholtz equation $\mathbf{L}w = 0$ for $\mathbf{x} \in \Omega_1$ and the Sommerfeld boundary conditions (2), but it no longer has to satisfy boundary conditions (9). The corresponding discontinuities at the interface Γ drive the surface control sources. The first term on the right-hand side of (10) represents the density of a single-layer potential, which is a layer of monopoles on the interface Γ, and the second term on the right-hand side of (10) represents the density of a double-layer potential, which is a layer of dipoles on the interface Γ. A detailed justification of formula (10) as general solution for surface controls can be found in [14], see also [4]. The fundamental properties of the surface controls (10) are the same as those of the volumetric controls (8).

In the family of surface controls (10) we identify two important particular cases. First, the cancellation of $u^-(\mathbf{x})$, $\mathbf{x} \in \Omega$, can be achieved by using surface monopoles only, i.e., by employing only a single-layer potential as the annihilating signal (anti-sound). To do that, we need to find $w(\mathbf{x})$, $\mathbf{x} \in \Omega_1$, such that there may be no discontinuity on Γ between $u(\mathbf{x})$ and $w(\mathbf{x})$, i.e., in the function itself, and the discontinuity may only "reside" in the normal derivative (see formula (10)). This $w(\mathbf{x})$ will obviously be a solution of the following external Dirichlet problem:

$$\mathbf{L}w = 0, \quad \mathbf{x} \in \Omega_1, \qquad w|_\Gamma = u|_\Gamma, \tag{11}$$

subject to the appropriate Sommerfeld boundary conditions (2). Problem (11) is uniquely solvable on $\Omega_1 = \mathbb{R}^n \backslash \overline{\Omega}$. Second, one can employ only the double-layer potential, i.e., use only surface dipoles as the control sources. The corresponding $w(\mathbf{x})$, $\mathbf{x} \in \Omega_1$, should then solve the external Neumann problem:

$$\mathbf{L}w = 0, \quad \mathbf{x} \in \Omega_1, \qquad \frac{\partial w}{\partial \mathbf{n}}\Big|_\Gamma = \frac{\partial u}{\partial \mathbf{n}}\Big|_\Gamma,$$

again, subject to the appropriate Sommerfeld conditions at infinity (2).

Altogether, we have introduced two different types of active controls on the surface and only one type—monopoles—in the volume. This is not accidental. In [4], we show that surface monopoles and dipoles provide different types of excitation to the surrounding sound-conducting medium, which warrants their separate consideration. At the same time, any volumetric distribution of dipoles can be recast into an equivalent volumetric distribution of monopoles, which effectively renders the volumetric dipoles superfluous, see [4].

Let us also note that in practice it may often be convenient to use the so-called *artificial boundary conditions* (ABCs), see the review [13], as a part of the definition of the auxiliary function $w(\mathbf{x})$. Assume that there is a larger domain that fully contains Ω and require, in addition, that $\mathbf{L}w = 0$ outside this

larger domain. This requirement implies that the resulting volumetric controls will be compactly supported between Γ and the outer boundary of the aforementioned larger region, see formula (8). From the standpoint of computing this is the only feasible way to obtain a finite discretization (see Section 2.2). In [4], we have obtained the ABCs for the homogeneous Helmholtz equation outside a sphere of radius R in 3D using the separation of variables in spherical coordinates and the appropriate mode selection:

$$\left.\frac{\mathrm{d}\hat{w}_{lm}}{\mathrm{d}\rho}\right|_{\rho=R} = \frac{\frac{\mathrm{d}}{\mathrm{d}\rho}[\rho^{-1/2}H^{(2)}_{l+1/2}(k\rho)]}{\rho^{-1/2}H^{(2)}_{l+1/2}(k\rho)}\hat{w}_{lm}(\rho)|_{\rho=R}. \tag{12}$$

In formula (12), ρ is the spherical radius, $\hat{w}_{lm}$ are the Fourier coefficients of $w(\mathbf{x})$ with respect to spherical functions Y^m_l, $l = 0, 1, 2, \ldots$, $m = 0, \pm 1, \ldots, \pm l$, and $H^{(2)}_{l+1/2}$ are Hankel's functions of the second kind; equalities (12) have to be enforced for all l and m. Similarly, for the homogeneous Helmholtz equation outside a disk of radius R in 2D, the ABCs from [4] read:

$$\left.\frac{\mathrm{d}\hat{w}_{l}}{\mathrm{d}\rho}\right|_{\rho=R} = \frac{\frac{\mathrm{d}}{\mathrm{d}\rho}H^{(2)}_{l}(k\rho)}{H^{(2)}_{l}(k\rho)}\hat{w}_{l}(\rho)|_{\rho=R}, \tag{13}$$

where ρ is the polar radius, and $\hat{w}_l$ are the Fourier coefficients of $w(\mathbf{x})$ with respect to the complex exponents $e^{-il\theta}$, $l = 0, \pm 1, \pm 2, \ldots$; again, equalities (13) have to be enforced for all l.

2.2. Discrete formulation of the problem

The continuous analysis tools employed for obtaining the control sources of the previous Section 2.1 are obviously deficient from the standpoint of applications. Indeed, any practical design of a noise control system can only be composed of a finite number of elements (sensors for measuring the field and actuators for creating the appropriate excitation, i.e., anti-sound). Therefore, it is natural to discretize the problem on the grid and obtain the control sources in the discrete framework so that the locations of the sensors and actuators can be associated with the grid nodes. For details regarding the discrete formulation of the problem we refer the reader to the monograph [12, Part VIII], as well as to the papers [16,17]; a brief account can also be found in [14,4], and below we summarize the results. Note that our discrete analysis is not limited to any specific type of the grid. In particular, no grid fitting to either the shape of the protected region Ω or that of the external artificial boundary, is generally required. However, for the purpose of illustrating the concepts discussed hereafter, we will use a two-dimensional example that involves a polar grid. The use of the polar grid greatly facilitates setting the discrete ABCs at the circular outer boundary of radius R. Moreover, the same two-dimensional polar example is analyzed later in Section 3 in the context of L_2 optimization.

Let us denote the aforementioned polar grid $\mathbb{N}$; it spans both Ω and Ω_1. Of course, the grid does not extend all the way to infinity, it is rather truncated by the external artificial boundary in the shape of a large circle of radius R. This, in particular, implies that the discrete control sources that we obtain will always be compactly supported. Assume that the grid has J cells in the radial direction with the nodes $\rho_j = j\Delta\rho$, $j = 0, \ldots, J$, so that $\rho_0 = 0$ and $\rho_J = R$; and L cells in the circumferential direction with the nodes $\theta_s = s\Delta\theta$, $s = 0, \ldots, L$, so that $\theta_0 = 0$ and $\theta_L = 2\pi$. For simplicity, it is convenient to think that the grid sizes $\Delta\rho = R/J$ and $\Delta\theta = 2\pi/L$ are constant; in applications, however, the grid in the radial direction may be stretched.

Let now $u^{(h)}$ be the acoustic field on the grid, and $\mathbf{L}^{(h)}$ be a finite-difference approximation of the differential operator $\mathbf{L}$ of (1). To accurately define the approximation, we will need to introduce another grid $\mathbb{M}$ along with the previously defined $\mathbb{N}$. On the grid $\mathbb{M}$, we will consider the residuals of $\mathbf{L}^{(h)}u^{(h)}$, and subsequently the right-hand sides to the corresponding discrete inhomogeneous equation. We will use the notations n and m for the individual nodes of the grids $\mathbb{N}$ and $\mathbb{M}$, respectively, and the notation $\mathbb{N}_m$ for the stencil of the discrete operator $\mathbf{L}^{(h)}$ centered at a given node $m \in \mathbb{M}$, so that

$$\mathbf{L}^{(h)}u^{(h)}|_m = \sum_{n\in\mathbb{N}_m} a_{mn}u_n^{(h)}, \tag{14}$$

where a_{nm} are the coefficients associated with particular nodes of the stencil. Generally, there are no limitations to the type of the discrete operator that one can use. We only require that the difference operator $\mathbf{L}^{(h)}$ of (14) approximate the differential operator $\mathbf{L}$ of (1) with the accuracy sufficient for a particular application. For the specific example that we are analyzing, we will consider a conventional second-order central-difference approximation, so that $\{m = (s, j)\} = \mathbb{M} \subset \mathbb{N} = \{n = (s, j)\}$. Then, formula (14) becomes:

$$\begin{aligned}\mathbf{L}^{(h)}u^{(h)}|_{s,j} \equiv{}& \frac{1}{\rho_j}\frac{1}{\Delta\rho}\left(\rho_{j+1/2}\frac{u_{s,j+1}^{(h)}-u_{s,j}^{(h)}}{\Delta\rho} - \rho_{j-1/2}\frac{u_{s,j}^{(h)}-u_{s,j-1}^{(h)}}{\Delta\rho}\right)\\ &+ \frac{1}{\rho_j^2}\frac{u_{s+1,j}^{(h)}-2u_{s,j}^{(h)}+u_{s-1,j}^{(h)}}{\Delta\theta^2} + k^2u_{s,j}^{(h)}.\end{aligned} \tag{15}$$

Next, we introduce subsets of the grids $\mathbb{M}$ and $\mathbb{N}$, which will allow us to accurately distinguish between the interior and exterior domains, sources, and solutions on the discrete level:

$$\begin{aligned}&\mathbb{M}^+ = \mathbb{M}\cap\Omega, \qquad \mathbb{M}^- = \mathbb{M}\backslash\mathbb{M}^+ = \mathbb{M}\cap\Omega_1,\\ &\mathbb{N}^+ = \bigcup_{m\in\mathbb{M}^+}\mathbb{N}_m, \qquad \mathbb{N}^- = \bigcup_{m\in\mathbb{M}^-}\mathbb{N}_m,\\ &\gamma = \mathbb{N}^+\cap\mathbb{N}^-, \qquad \gamma^+ = \mathbb{N}^-\cap\Omega, \qquad \gamma^- = \mathbb{N}^+\cap\Omega_1.\end{aligned} \tag{16}$$

Note that whereas the residuals' grid $\mathbb{M}$ is partitioned into $\mathbb{M}^+$ and $\mathbb{M}^-$ directly, the subgrids $\mathbb{N}^+$ and $\mathbb{N}^-$ are rather obtained by applying the stencil $\mathbb{N}_m$ to all the nodes of $\mathbb{M}^+$ and $\mathbb{M}^-$, respectively. As such, $\mathbb{N}^+$ and $\mathbb{N}^-$ do overlap. Their overlap is denoted by $\gamma = \gamma^+\cup\gamma^-$, see (16), and is called *the grid boundary*; it is a fringe of nodes that is located near the continuous boundary Γ and in some sense straddles it. For the polar second-order Laplacian $\mathbf{L}^{(h)}$ (15), the grid boundary γ will be a two-layer fringe of grid nodes around Γ, as shown schematically in Fig. 2.

The discrete noise control problem is formulated similarly to the continuous one, see Section 1. Let $f_m^{(h)+}$, $m \in \mathbb{M}^+$, and $f_m^{(h)-}$, $m \in \mathbb{M}^-$, be the interior and exterior discrete acoustic sources, respectively. Let $u_n^{(h)+}$, $n \in \mathbb{N}$, and $u_n^{(h)-}$, $n \in \mathbb{N}$, be the corresponding solutions, i.e., $\mathbf{L}^{(h)}u^{(h)+} = f^{(h)+}$ and $\mathbf{L}^{(h)}u^{(h)-} = f^{(h)-}$. Using the same terminology as before, we will call $u^{(h)+}$ the discrete sound and $u^{(h)-}$ the discrete noise. The overall discrete acoustic field $u^{(h)}$ is the sum of its sound and noise components, $u^{(h)} = u^{(h)+} + u^{(h)-}$ on $\mathbb{N}$, and it obviously satisfies the equation $\mathbf{L}^{(h)}u^{(h)} = f^{(h)} \equiv f^{(h)+} + f^{(h)-}$. The goal is to obtain the discrete control sources $g^{(h)} = g_m^{(h)}$ so that the solution $\tilde{u}^{(h)}$ of the equation $\mathbf{L}^{(h)}\tilde{u}^{(h)} = f^{(h)+} + f^{(h)-} + g^{(h)}$ be equal to only the sound component $u^{(h)+}$ on the sub-grid $\mathbb{N}^+$.

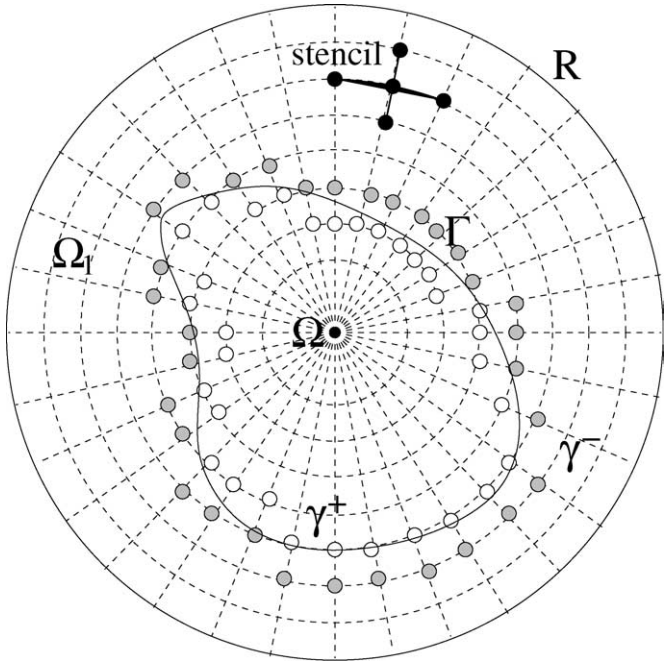

Fig. 2. Schematic geometry of the domains, the stencil, and the grid boundary $\gamma = \gamma^+ \cup \gamma^-$ in polar coordinates: Hollow bullets denote γ^+, filled bullets—γ^-.

A general solution for the discrete control sources $g^{(h)} = g_m^{(h)}$ that eliminate the unwanted noise $u^{(h)-}$ on $\mathbb{N}^+$ is given by the following formula (cf. (8)):

$$g_m^{(h)} = -\mathbf{L}^{(h)} w^{(h)}|_{m\in\mathbb{M}^-}, \tag{17}$$

where $w^{(h)} = w_n^{(h)}$, $n \in \mathbb{N}^-$, is a discrete auxiliary function-parameter. The requirements that it must satisfy are, again, rather "loose", and can be considered natural discrete analogues of the corresponding continuous requirements for the function-parameter $w(\mathbf{x})$. Namely, at the grid boundary γ the function $w^{(h)}$ has to coincide with the overall acoustic field $u^{(h)}$ to be controlled:

$$w_n^{(h)}|_{n\in\gamma} = u_n^{(h)}|_{n\in\gamma}. \tag{18}$$

For practical designs, the boundary data $u_n^{(h)}|_{n\in\gamma}$ shall be interpreted as measurable quantities that provide input for the control system. In other words, we can think of a microphone at every node of γ that measure the characteristics of the actual acoustic field and generate the input signal $u_n^{(h)}|_{n\in\gamma}$.

The other requirement of the function $w^{(h)}$, besides the interface boundary conditions (18), is that it must satisfy the appropriate discrete ABCs at the external artificial boundary $\rho = R$, see Fig. 2. The role of the discrete ABCs is the same as that of the continuous ABCs—to provide a replacement for the Sommerfeld radiation boundary conditions. The discrete two-dimensional ABCs were obtained in [4] by using the direct and inverse discrete Fourier transforms, $l = -L/2+1, \ldots, L/2$, $s = 0, \ldots, L-1$:

$$\hat{w}_l = \frac{1}{L}\sum_{s=0}^{L-1} w_s e^{-ils\Delta\theta}, \qquad w_s = \sum_{l=-L/2+1}^{L/2} \hat{w}_l e^{ils\Delta\theta}, \tag{19}$$

and then approximating boundary conditions (13) for $l = -L/2+1, \ldots, L/2$ with the second order of accuracy:

$$\frac{\hat{w}_{l,J} - \hat{w}_{l,J-1}}{\Delta\rho} - \beta_l \frac{\hat{w}_{l,J} + \hat{w}_{l,J-1}}{2} = 0,$$
$$\beta_l = \left.\frac{\frac{\mathrm{d}}{\mathrm{d}\rho} H^{(2)}_{\alpha_l}(k\rho)}{H^{(2)}_{\alpha_l}(k\rho)}\right|_{\rho=R}, \qquad \alpha_l^2 = \frac{4}{\Delta\theta^2}\sin^2\frac{l\Delta\theta}{2}. \tag{20}$$

Note, $-\alpha_l^2$ of (20) are eigenvalues of the circumferential component of the discrete Laplacian (15). Relations (20) for all $l = -L/2+1, \ldots, L/2$ can also be recast into the matrix form:

$$\mathbf{w}_{\cdot,J} = \mathbf{F}^{-1}\,\mathrm{diag}\left\{-\left(\frac{1}{\Delta\rho} + \beta_l\right)\left(\frac{1}{\Delta\rho} - \beta_l\right)^{-1}\right\}\mathbf{F}\,\mathbf{w}_{\cdot,J-1} \equiv \mathbf{T}\,\mathbf{w}_{\cdot,J-1}, \tag{21}$$

where $\mathbf{F}$ and $\mathbf{F}^{-1}$ are matrices of the direct and inverse discrete Fourier transforms of (19), and $\mathbf{w}_{\cdot,J}$ and $\mathbf{w}_{\cdot,J-1}$ are L-dimensional vectors of components $w^{(h)}_{s,J}$ and $w^{(h)}_{s,J-1}$, respectively, $s = 0, 1, \ldots, L-1$.

Other than (18) and (21), there are no constraints on $w^{(h)}$. As such, it parameterizes a large variety of discrete control sources, see (17), that will provide the search space for optimization in Section 3.

It is also important to understand in what sense this discrete cancellation of noise models the continuous cancellation described in Section 2. According to the theory of generalized Calderon's potentials, see [12], the discrete anti-sound $v^{(h)} = v^{(h)}_n$, $n \in \mathbb{N}^+$, i.e., the solution to $\mathbf{L}^{(h)}v^{(h)} = g^{(h)}$ with $g^{(h)}$ given by (17), will, under certain natural conditions, approximate the continuous anti-sound $v = v(\mathbf{x})$, $\mathbf{x} \in \Omega$, i.e., the solution to $\mathbf{L}v = g$ with g given by (8). The aforementioned conditions first include the consistency and stability of the finite-difference scheme for the Helmholtz equation. In addition, the discrete boundary data $u^{(h)}_n|_{n\in\gamma}$ of (18) have to approximate the continuous boundary data $(u, \frac{\partial u}{\partial \mathbf{n}})|_\Gamma$ of (9) in some special sense, [12]. Then, the rate of convergence of the discrete anti-sound to the continuous one with respect to h will be the same as prescribed by the finite-difference scheme itself. For the central-difference operator (15), this rate is $\mathrm{O}(h^2)$. In other words, when designing an active control system following the finite-difference approach, one can expect to have the actual noise cancellation in the same approximate sense as the solution of the finite-difference equation approximates the corresponding solution of the original differential equation.

Finally, similarly to the continuous case we can identify some particular types of the discrete control sources. First, let us define another subset of the grid $\mathbb{M}$ (more precisely, of $\mathbb{M}^-$):

$$\mathbb{M}^-_{\mathrm{int}} = \left\{m \in \mathbb{M}^- \mid \mathbb{N}_m \cap \gamma^+ = \emptyset\right\}.$$

Basically, $\mathbb{M}^-_{\mathrm{int}}$ is the interior subset of $\mathbb{M}^-$, such that when the center of the stencil sweeps this subset, the stencil itself does not touch γ^+, see Fig. 2. In other words, $\mathbb{M}^-_{\mathrm{int}}$ is a subset of $\mathbb{M}^-$ such that

$$\bigcup_{m\in\mathbb{M}^-_{\mathrm{int}}} \mathbb{N}_m = \mathbb{N}^- \backslash \gamma^+.$$

Next, we introduce $w^{(h)} = w^{(h)}_n$, $n \in \mathbb{N}^-$, for (17) as follows:

$$w^{(h)}_n|_{n\in\gamma^+} = u^{(h)}_n|_{n\in\gamma^+}, \tag{22a}$$

and

$$w^{(h)}_n|_{n\in\gamma^-} = u^{(h)}_n|_{n\in\gamma^-}, \qquad \mathbf{L}^{(h)}w^{(h)} = 0 \quad \text{on } \mathbb{M}^-_{\mathrm{int}}. \tag{22b}$$

As before, we also assume that $w^{(h)}$ satisfies the discrete ABCs (21). Definition (22a) means that on the interior part of the grid boundary γ^+ we simply set $w^{(h)}$ equal to the given $u^{(h)}$: $w_n^{(h)}|_{n\in\gamma^+} = u_n^{(h)}|_{n\in\gamma^+}$. Definition (22b) is actually a discrete exterior boundary-value problem of the Dirichlet type. Indeed, everywhere on and "outside" the exterior part of the grid boundary γ^-, i.e., on $\mathbb{N}^-\backslash\gamma^+$, the grid function $w^{(h)}$ is obtained as a solution of the homogeneous equation $\mathbf{L}^{(h)}w^{(h)} = 0$ (enforced at the nodes $\mathbb{M}^-_{\text{int}}$) supplemented by the Dirichlet boundary data on γ^-: $w_n^{(h)}|_{n\in\gamma^-} = u_n^{(h)}|_{n\in\gamma^-}$. Note, relation (22a) and the first relation (22b) together are obviously equivalent to (18). Therefore, the function $w^{(h)}$ defined via (22a), (22b) falls into the general class of $w^{(h)}$'s used for obtaining the discrete control sources (17).

Problem (22b) can clearly be considered a finite-difference counterpart to the continuous Dirichlet problem (11). Therefore, its is natural to call the control sources $g^{(h)} \equiv g^{(\text{h,surf})}_{\text{monopole}}$ obtained by formulae (17), (22a), (22b) *the discrete surface monopoles*. Indeed, because of the definition of $w^{(h)}$ given by (22a) and (22b), these $g^{(\text{h,surf})}_{\text{monopole}}$ may, generally speaking, differ from zero only on the grid set $\mathbb{M}^-\backslash\mathbb{M}^-_{\text{int}}$, which is a single "curvilinear" layer of nodes of grid $\mathbb{M}$ that follows the geometry of Γ. Accordingly, the output of these controls can be called the discrete single-layer potential. Note, the discrete surface monopoles and single-layer potentials, as well as the discrete surface dipoles and double-layer potentials, have been first introduced and analyzed in [14].

3. Optimization of the control sources

Once the general solution for controls is available, in either continuous (8) or discrete (17) formulation, the next step is to determine what particular element of this large family of functions will be optimal for a specific setting. There is a multitude of possible criteria for optimality that one can use. In many practical problems the cancellation of noise is only approximate and as such, the key criterion for optimization (or sometimes, the key constraint) is the quality of this cancellation, i.e., the extent of noise reduction. In contradistinction to that, in this paper we are considering ideal, or exact, cancellation, i.e., every particular control field from either the continuous (8) or discrete (17) family completely eliminates the unwanted noise on the domain of interest. Consequently, the criteria for optimality that we can employ will not include the level of the residual noise as a part of the corresponding function of merit, and should rather depend only on the control sources themselves.

In the current paper we focus primarily on the *quadratic optimization criteria.* We have looked into the most natural criterion of this type, namely, the L_2 norm of the control sources $g(\mathbf{x})$ of (8) or $g_m^{(h)}$ of (17), see Section 3.2. The advantage of minimizing the controls in the sense of L_2:

$$\|g\|_2 \equiv \sqrt{\int\limits_{\text{supp}\, g} \left|g(\mathbf{x})\right|^2 \mathrm{d}\mathbf{x}} \to \min \tag{23}$$

is that *the minimum can be easily computed*, see Section 3.2. The search space for minimization (23) includes all the appropriate auxiliary functions $w(\mathbf{x})$, on which $g(\mathbf{x})$ depends. The disadvantage of using this criterion is that the quantity $\|g\|_2$ does not have a clear physical interpretation, as, for example, the L_1 norm of g (see Section 3.1 and [4]) or the power required by the control system (see [5]) do. Nonetheless, motivated primarily by the ease of the numerical approach to minimization, we do provide in Section 3.2 a comprehensive set of computed optimal solutions for active controls in the sense of the least squares

(i.e., L_2). We also compare these discrete results with the "semi-analytic" L_2 optimal solutions obtained for simple circular shapes using the spectral methodology developed in our work [6].

The discrete L_2 minimization problem for the control sources $g^{(h)}$ of (17) can be formulated as follows:

$$\left\| g^{(h)} \right\|_2 \equiv \sqrt{\sum_{m \in \mathbb{M}^-} V_m \left| g_m^{(h)} \right|^2} \to \min,$$

where V_m accounts for the grid cell area. This problem can also be recast using matrices. The finite-difference operator $\mathbf{L}^{(h)}$ can be interpreted as a matrix with N columns and M rows, where N is the number of nodes $n \equiv (s, j)$ of the grid $\mathbb{N}^-$ such that $\rho_j \leqslant R$, i.e., $j \leqslant J$, and M is the number of nodes $m \equiv (s, j)$ of the grid $\mathbb{M}^-$ such that $\rho_j < R$, i.e., $j \leqslant J - 1$. Let $\mathbf{w}$ be the vector of N components $w_n^{(h)} \equiv w_{s,j}^{(h)}$, $n \in \mathbb{N}^-$ and $j \leqslant J$, arranged so that

$$\mathbf{w} = [\mathbf{w}_\gamma, \mathbf{w}_0, \mathbf{w}_{\cdot,J-1}, \mathbf{w}_{\cdot,J}]^{\mathrm{T}}, \tag{24}$$

where $\mathbf{w}_\gamma$ contains $w_n^{(h)}$ for which $n \in \gamma$, $\mathbf{w}_{\cdot,J}$ and $\mathbf{w}_{\cdot,J-1}$ correspond to the outermost and second to last circles of the polar grid, respectively, as in formula (21), and $\mathbf{w}_0$ contains all the remaining components of $\mathbf{w}$ "in-between" γ and the outer boundary. In accordance with (24), the matrix $\mathbf{L}^{(h)}$ can be decomposed into four sub-matrices:

$$\mathbf{L}^{(h)} = [\mathbf{A}, \mathbf{B}, \mathbf{C}, \mathbf{D}] \tag{25}$$

that all have the same number of rows M, and $\mathbf{A}$ has as many columns as there are nodes in γ (we denote this number $|\gamma|$), while $\mathbf{C}$ and $\mathbf{D}$ each has L columns, and $\mathbf{B}$ has $N - |\gamma| - 2L$ columns.

With the help of formulae (24) and (25) the discrete minimization problem can now be formulated as:

$$\left\| \mathbf{V}(\mathbf{A}\mathbf{w}_\gamma + \mathbf{B}\mathbf{w}_0 + \mathbf{C}\mathbf{w}_{\cdot,J-1} + \mathbf{D}\mathbf{w}_{\cdot,J}) \right\|_2 \to \min, \tag{26}$$

where $\mathbf{V}$ is an $M \times M$ diagonal matrix with the entries given by the corresponding cell areas V_m. The vector $\mathbf{w}$ in (26) is, in fact, subject to a number of equality-type constraints that come from the interface conditions (18) and ABCs (21). More precisely, the first sub-vector $\mathbf{w}_\gamma$ in (24) is known and fixed because of (18) and we can rewrite (18) as $\mathbf{w}_\gamma = \mathbf{u}_\gamma$, where $\mathbf{u}_\gamma$ is given. The last sub-vector $\mathbf{w}_{\cdot,J}$ in (24) is a function of $\mathbf{w}_{\cdot,J-1}$ according to (21). Therefore, we can conclude that only $\mathbf{w}_0$ and $\mathbf{w}_{\cdot,J-1}$ contain free variables that provide the search space for optimization, and as such recast (26) as

$$\min_{\mathbf{w}_0, \mathbf{w}_{\cdot,J-1}} \left\| \mathbf{V}\big(\mathbf{B}\mathbf{w}_0 + (\mathbf{C} + \mathbf{D}\mathbf{T})\mathbf{w}_{\cdot,J-1} + \mathbf{A}\mathbf{w}_\gamma\big) \right\|_2 \equiv \min_{\mathbf{z}} \|\mathbf{E}\mathbf{z} - \mathbf{f}\|_2, \tag{27}$$

where $\mathbf{E} = \mathbf{V}[\mathbf{B}, \mathbf{C} + \mathbf{D}\mathbf{T}]$ is an $M \times (N - |\gamma| - L)$ given matrix, $\mathbf{z} = [\mathbf{w}_0, \mathbf{w}_{\cdot,J-1}]^{\mathrm{T}}$ is an $(N - |\gamma| - L)$-dimensional vector of unknowns, and $\mathbf{f} = -\mathbf{V}\mathbf{A}\mathbf{w}_\gamma$ is an M-dimensional known vector of the right-hand side.

3.1. Results of optimization in the sense of L_1

Before actually solving problem (27) let us briefly outline here our recent results [4] on finding the optimal controls is the sense of L_1. These results will serve as a good "reference point" for comparison in the context of the current paper. Minimization problem in the sense of L_1:

$$\|g\|_1 \equiv \int_{\operatorname{supp} g} \left| g(\mathbf{x}) \right| \mathrm{d}\mathbf{x} \to \min,$$

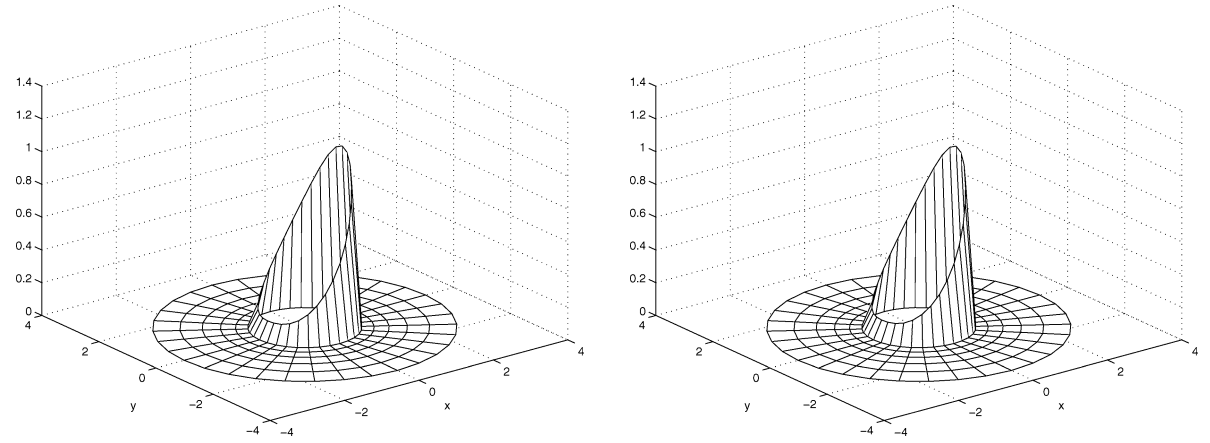

Fig. 3. Magnitude of the control sources for $\Omega = \{\mathbf{x} \in \mathbb{R}^2 \mid |\mathbf{x}| < 1\}$, $k = 0.5$, $f^- = \delta(\mathbf{x} - \mathbf{x}_1)$, $\mathbf{x}_1 = (5, 0)$; grid dimension 32×7: (a) L_1 optimal solution; (b) Surface monopoles $g^{(\mathrm{h,surf})}_{\mathrm{monopole}}$.

is formulated analogously to that in the sense of L_2, see (23), and also has a matrix representation similar to (27) except that the norm $\|\cdot\|_2$ shall be replaced by $\|\cdot\|_1$. From the standpoint of physics, the L_1 minimization is equivalent to minimizing *the overall absolute acoustic source strength* of the control sources $g(\mathbf{x})$, see [8,7]. The transparent physical meaning of the cost function $\|g\|_1$ is, undoubtedly, an advantage. On the other hand, because of the complex-valued quantities involved, the computation of $\min \|g\|_1$ reduces to solving a nonlinear and nonsmooth problem of constrained optimization over a large set of cones, see [4]. It presents a substantial challenge even for the most sophisticated state-of-the-art approaches to numerical optimization based on the interior point methods [15,9]. For computing the L_1 optima in [4] we have used the software package SeDuMi by J.F. Sturm.[2]

The key computational finding of [4] is that the L_1 optimal solution always coincides with the discrete layer of surface monopoles $g^{(\mathrm{h,surf})}_{\mathrm{monopole}}$ obtained by applying formula (17) to the auxiliary function $w^{(h)}$ defined by (22a), (22b). Fig. 3 reproduces the results of one particular computation from [4]. Motivated by the consistent numerical observations, we have also been able to prove in [4] that in 1D the surface monopoles indeed provide a global minimum for the control sources in the sense of L_1 for both the discrete and continuous formulation of the problem. In multi-D, this result is still a conjecture, even though we do believe that a combination of the two-dimensional numerical evidence and a one-dimensional rigorous proof, see [4], cannot be a mere coincidence. To accurately formulate this conjecture from [4], we first remind that according to (10) the continuous surface monopole controls are given by

$$g^{(\mathrm{surf})}_{\mathrm{monopole}}(\mathbf{x}) = -\left[\frac{\partial w_D}{\partial \mathbf{n}} - \frac{\partial u}{\partial \mathbf{n}}\right]_{\Gamma} \delta(\Gamma) \equiv \nu(\mathbf{x})|_{\mathbf{x}\in\Gamma} \cdot \delta(\Gamma), \tag{28}$$

where $w_D(\mathbf{x})$ is a solution to the exterior Dirichlet problem (11). Then,

Conjecture 3.1. Let a complex-valued function $w = w(\mathbf{x})$ be defined on $\Omega_1 = \mathbb{R}^n \backslash \overline{\Omega}$, and let it be sufficiently smooth so that the operator $\mathbf{L}$ of (1) can be applied to $w(\mathbf{x})$ on its entire domain in the

[2] http://fewcal.kub.nl/sturm/software/sedumi.html.

classical sense, and the result $\mathbf{L}w$ be locally absolutely integrable, $\mathbf{L}w \in L_1^{(\mathrm{loc})}(\mathbb{R}^n)$. Let, in addition, $w(\mathbf{x})$ satisfy the interface conditions (9), where $u = u(\mathbf{x})$ is a given field to be controlled, and the appropriate Sommerfeld radiation boundary conditions at infinity (2). Then, the greatest lower bound for the L_1 norms of all the control sources $g(\mathbf{x})$ obtained with such auxiliary functions $w(\mathbf{x})$ using formula (8), is given by the L_1 norm on Γ of the magnitude of surface monopoles (28):

$$\inf_{w(\mathbf{x})} \int_{\Omega_1} \bigl|g(\mathbf{x})\bigr| \,\mathrm{d}\mathbf{x} = \int_{\Gamma} \bigl|\nu(\mathbf{x})\bigr| \,\mathrm{d}s.$$

In other words, we have $\inf_{w(\mathbf{x})} \|g(\mathbf{x})\|_{1,\Omega_1} = \|\nu\|_{1,\Gamma}$. Note that in the discrete case the L_1 optimal solution $g^{(\mathrm{h,surf})}_{\mathrm{monopole}}$ belongs to the same class of functions as all other discrete volumetric controls $g_m^{(h)}$ do, whereas the continuous optimum (28) of the controls $g(\mathbf{x}) \in L_1^{(\mathrm{loc})}$ happens to be a singular layer.

3.2. Discrete optimization in the sense of L_2

The L_2 minimization problem for the volumetric control sources is solved hereafter completely on the discrete level. In other words, for every particular setup we are finding the minimum (27) or, equivalently, computing a complex-valued weak solution of the overdetermined system of linear equations $\mathbf{Ez} = \mathbf{f}$ in the sense of the least squares. The resulting optima do not reduce to any clearly identifiable special cases, like the layer of surface monopoles that appeared previously in the context of L_1. They are not assigned any particular physical meaning either; and we present them below in order to demonstrate that the L_2 optima are distinctly different from the L_1 optima obtained in [4], and that they can be easily computed numerically, including some cases that involve rather sophisticated geometry. In the simple case of Ω being a disk, we also conduct a grid convergence study in order to validate the results of the discrete L_2 minimization against the spectrally accurate reference solutions obtained in [6].

Proposition 1. *The matrix* $\mathbf{E} = \mathbf{V}[\mathbf{B}, \mathbf{C} + \mathbf{DT}]$, *see formulae* (25), (27), *has full column rank.*

Proof. The justification of Proposition 1 will be based on a natural solvability assumption for the system of finite-difference equations that we are using. First, let us introduce more detailed partitions of $\mathbf{w}$ and $\mathbf{L}^{(h)}$ instead of (24) and (25), respectively:

$$\begin{aligned} &\mathbf{w} = [\mathbf{w}_{\gamma^+}, \mathbf{w}_{\gamma^-}, \mathbf{w}_0, \mathbf{w}_{\cdot,J-1}, \mathbf{w}_{\cdot,J}]^{\mathrm{T}}, \\ &\mathbf{L}^{(h)} = [\mathbf{A}^+, \mathbf{A}^-, \mathbf{B}, \mathbf{C}, \mathbf{D}]. \end{aligned} \tag{29}$$

The matrices $\mathbf{A}^+$ and $\mathbf{A}^-$ of (29) together give $\mathbf{A}$ of (25); $\mathbf{w}_{\gamma^+}$ and $\mathbf{A}^+$ correspond to the innermost "half" of the grid boundary γ^+, and $\mathbf{w}_{\gamma^-}$ and $\mathbf{A}^-$ correspond to the outermost "half" of the grid boundary γ^- (see formula (16) and Fig. 2). Next, consider an auxiliary exterior Dirichlet problem for the finite-difference equation $\mathbf{L}^{(h)} z^{(h)} = 0$ with the boundary data specified at γ^+. As before, the problem is supposed to be truncated at the external artificial boundary $\rho = \rho_J$ by means of the ABC (21). This problem is a discrete counterpart of the continuous exterior Dirichlet problem for the Helmholtz equation with the boundary data given at Γ and ABCs (13) specified at $\rho = R$. The continuous problem is uniquely solvable because it is equivalent to the genuine infinite-domain exterior Dirichlet problem with the Sommerfeld boundary conditions (2) set at infinity. Even though we do not justify it here, it is

certainly reasonable to assume that the corresponding discrete problem based on the standard central-difference scheme (15) and ABC (21) is uniquely solvable as well.[3] The latter assumption implies that the square $M \times M$ matrix $[\mathbf{A}^-, \mathbf{B}, \mathbf{C} + \mathbf{DT}]$, see formula (29), is nonsingular. Consequently, the matrix $\mathbf{G} = \mathbf{V}[\mathbf{A}^-, \mathbf{B}, \mathbf{C} + \mathbf{DT}]$ is also nonsingular, because $\mathbf{V}$ is an $M \times M$ diagonal matrix with nonzero diagonal entries V_m. Finally, we notice that the matrix $\mathbf{E} = \mathbf{V}[\mathbf{B}, \mathbf{C} + \mathbf{DT}]$, see formulae (24) and (25), is obtained by removing the first $|\gamma^-|$ columns of the previous matrix $\mathbf{G}$. Therefore, the columns of $\mathbf{E}$ are linearly independent. □

An obvious key implication of Proposition 1 is that the minimization problem (26), or equivalently (27), can be solved in the sense of L_2 (least squares) using a standard QR-based approach, i.e., without employing the Moore–Penrose type arguments. We use the MATLAB function `LSQLIN` for solving the least squares minimization problems hereafter. This function also allows one to do constrained minimization, the capability that we employ in Section 3.2.2.

3.2.1. Comparison with the reference solution

In our previous work [6] we have developed a methodology of spectral type that allowed us to construct the continuous L_2-optimal volumetric controls for a particular geometry, namely, controls supported on annular domains. These spectral solutions are used in the current paper as reference solutions for the purpose of validating the finite-difference algorithm.

Let the protected region be a disk of radius r centered at the origin: $\Omega = \{(\rho, \theta) \mid \rho < r\}$, and let the controls be supported on the annulus $\Omega_1 = \{(\rho, \theta) \mid r \leqslant \rho \leqslant R\}$. We introduce a simple conformal polar grid, which is uniform in the circumferential direction and stretched in the radial direction so that the cell aspect ratio is equal to one:

$$\mathbb{M} = \big\{(\rho_j, \theta_s) \mid \rho_j = e^{j\Delta\theta},\ j = 0, \ldots, J-1;\ \theta_s = s\Delta\theta,\ s = 0, \ldots, L-1;\ \Delta\theta = 2\pi/L\big\},$$
$$\mathbb{N} = \big\{(\rho_j, \theta_s) \mid \rho_j = e^{j\Delta\theta},\ j = -1, 0, \ldots, J;\ \theta_s = s\Delta\theta,\ s = 0, \ldots, L-1;\ \Delta\theta = 2\pi/L\big\}. \tag{30}$$

We, of course, assume that the area covered by the grid $\mathbb{N}$ of (30) is larger than Ω_1, i.e., $\rho_{-1} < r < R < \rho_J$. The Helmholtz operator can be easily approximated on the grid (30) with the second order of accuracy using the same five-node stencil as shown in Fig. 2. This approximation involves only minor changes compared to the approximation (15) that works on uniform grids, and we refer the reader to our paper [10] for detail. The discrete ABCs in the form (20) or (21) do not change, except that $\Delta\rho$ needs to be replaced by $\Delta\rho_J = \rho_J - \rho_{J-1}$. Let us also note that we do not consider the grid (30) inside the domain Ω because we introduce it only for the purpose of obtaining the control sources on Ω_1. If, however, we were to actually compute the output of the controls inside the protected region, we would have had to extend the grid (30) all the way into Ω, which can obviously be done using a variety of strategies. As indicated by the previous analysis [6,12,16,17], as long as the discrete controls are constructed according to formulae (17), (18), their output on the grid inside Ω will identically cancel out the unwanted acoustic

[3] A proof of this fact would involve showing that relations (20) are "sufficiently close" to guaranteeing the precise mode selection in the discrete case so that to avoid the resonances. This task is beyond the scope of the current paper. In [11], one can find general analysis of the 1D discrete solvability and well-posedness.

component $u^{(h)-}$, see Section 2.2. In all the cases analyzed hereafter, we have $\rho_{-1} < r \leqslant \rho_0$, so that according to (16) the grid subsets are defined as

$$\begin{aligned}
&\mathbb{M}^+ = \{(\rho_j, \theta_s) \mid j = -1\}, && \mathbb{M}^- = \{(\rho_j, \theta_s) \mid 0 \leqslant j \leqslant J-1\},\\
&\mathbb{N}^+ = \{(\rho_j, \theta_s) \mid j = -1, 0\}, && \mathbb{N}^- = \{(\rho_j, \theta_s) \mid -1 \leqslant j \leqslant J\},\\
&\gamma = \{(\rho_j, \theta_s) \mid j = -1, 0\}, && \gamma^+ = \{(\rho_j, \theta_s) \mid j = -1\}, \qquad \gamma^- = \{(\rho_j, \theta_s) \mid j = 0\},
\end{aligned} \tag{31}$$

where always $s = 0, \ldots, L-1$. In so doing, the dimension of the matrix $\mathbf{L}^{(h)}$, see (25), is $M \times N \equiv (L \cdot J) \times (L \cdot (J+2))$, the dimension of $\mathbf{A}$, which corresponds to the variables on γ, is $M \times 2 \cdot L \equiv (L \cdot J) \times 2 \cdot L$, the dimension of $\mathbf{B}$ is $M \times (N - 4L) \equiv (L \cdot J) \times (L \cdot (J-2))$, and the dimension of either $\mathbf{C}$ or $\mathbf{D}$ is $M \times L \equiv (L \cdot J) \times L$.

We test the convergence of the discrete scheme for the wavenumber $k = 1.0$ and the excitation (i.e., the acoustic field $u^{(h)}$ that drives the control system) taken in the analytic form of a shifted fundamental solution of the Helmholtz operator, as if it were generated by the point source $f^- = \delta(\mathbf{x} - \mathbf{x}_1)$, where $\mathbf{x}_1 = (\rho\cos\theta, \rho\sin\theta) = (5, 0)$. We reemphasize that our approach does not require the explicit knowledge of the exterior sources of noise. We only need this function $u^{(h)}$ as a sample field to be used as given data in formula (18).

We employ a sequence of seven grids: $L \times J = 32 \times 3$, 48×4, 64×5, 96×7, 128×9, 192×13, and 256×17, so that for all the grids the value of ρ_{J-1} is the same: $\rho_{J-1} = \text{const} \approx 1.481$; according to (30) we also have $\rho_0 = 1$. For the first series of convergence tests we assume that the boundaries $\rho = r$ and $\rho = R$ of the region Ω_1, on which the continuous controls are to be supported, are located exactly at the conformal midpoint of the first and last cell of the radial grid $\mathbb{N}$ of (30), respectively, i.e., $r = e^{-1/2\Delta\theta}$ and $R = e^{(J-1/2)\Delta\theta}$. The results of these tests are summarized in Table 1, which shows the L_2 norm of the relative error between the optimal continuous and discrete controls: $\arg[\min_{\mathbf{w}(\mathbf{x})} \|g_{\text{spect}}(\mathbf{x})\|_2]$ and $\arg[\min_{w^{(h)}} \|g^{(h)}\|_2^{(h)}]$.

The data in Table 1 clearly indicate the second order of grid convergence for the discrete optimal controls $g^{(h)}$. It is important to emphasize, though, that the geometry of Ω_1 was chosen grid dependent (boundaries $\rho = r$ and $\rho = R$ were located at cell midpoints), which essentially means that for each subsequent grid in Table 1 the optimum was computed on a somewhat different (smaller) domain. It is quite obvious that in general the optimal solution will depend on the region on which the optimization is performed, and we cannot expect the optimum computed on a subdomain to coincide with the corresponding fragment of the optimum computed on the entire domain. However, the decrease of the error with the refinement of the grid observed in Table 1 shall still be interpreted as convergence. Indeed, had we continued refining the grid further, all the domains $\Omega_1 = \{r \leqslant \rho \leqslant R\}$ themselves would converge to one and the same annular region with the inner radius $r = \rho_0 = 1$ (Ω is a unit disk) and outer radius $R = \rho_{J-1}$, which was chosen grid independent.

On the other hand, the quadratic rate of convergence suggested by Table 1 appears a rather fragile phenomenon determined by the particular choice of the geometry. For other choices, the convergence may be slower. In Table 2, we present the results that correspond to the same inner boundary $r = e^{-1/2\Delta\theta}$,

Table 1
Grid convergence for: $k = 1$, $f^- = \delta(\mathbf{x} - \mathbf{x}_1)$, $\mathbf{x}_1 = (5, 0)$, $r = e^{-1/2\Delta\theta}$, $R = e^{(J-1/2)\Delta\theta}$

Grid	32×3	48×4	64×5	96×7	128×9	192×13	256×17
$\|\text{Error}\|_2$	0.013722	0.0061417	0.0034693	0.0015491	0.00087349	0.00038921	0.00021922

Table 2
Relative L_2 error for: $k = 1$, $f^- = \delta(\mathbf{x} - \mathbf{x}_1)$, $\mathbf{x}_1 = (5, 0)$, $r = e^{-1/2\Delta\theta}$, $R = e^{(J-3/4)\Delta\theta}$ and $R = e^{(J-1/4)\Delta\theta}$

Grid	32×3	48×4	64×5	96×7	128×9	192×13	256×17
$J - \frac{3}{4}$	0.10283	0.074135	0.058274	0.040958	0.031618	0.021733	0.016562
$J - \frac{1}{4}$	0.096894	0.071804	0.057069	0.040476	0.031362	0.021627	0.016504

and the outer boundary located at either one quarter point or three quarters point of the outermost cell: $R = e^{(J-3/4)\Delta\theta}$ or $R = e^{(J-1/4)\Delta\theta}$. One can easily see that the convergence in Table 2 is only linear.

At the moment, we do not have a detailed explanation of the grid convergence properties for $g^{(h)}$ that we have observed, see Tables 1 and 2. It is important to realize, however, that what we evaluate is, in fact, convergence of the residual rather than that of the solution. Indeed, the solution of the optimization problem (26) or (27) per se is a particular grid function $w^{(h)}$ that delivers minimum to the selected function of merit, namely, the L_2 norm of the residual of the discrete Helmholtz operator applied to this $w^{(h)}$. What motivates our primary interest toward the residual is obviously the fact that it yields the distributed active control sources $g^{(h)}$, see formula (17). However, even though the optimization formulation that we have introduced in the beginning of Section 3 is fairly conventional, in the PDEs' perspective neither the continuous generating function $w(\mathbf{x})$ nor its discrete counterpart $w^{(h)}$ at the optimum can, to the best of our knowledge, be interpreted as a solution to any traditional boundary-value problem, for which the existence and regularity results are available. As such, in our opinion no standard theoretical approaches to analyzing the grid convergence of either $w^{(h)}$ or its residual will directly apply here, and we shall rather regard the foregoing results as experimental findings.

Moreover, let us point out that in the context of noise cancellation on the domain Ω, the issue of grid convergence of the discrete control sources $g^{(h)}$ may, in some sense, be considered as the one of secondary importance. Indeed, the output of the controls $g^{(h)}$ always eliminates the unwanted noise on Ω [more precisely, on the grid $\mathbb{N}^+$, see formula (16)] no matter what particular solution from the general class (17), (18) is used. Moreover, this output on $\mathbb{N}^+$ can be interpreted as a discrete Calderon's potential, which converges to its continuous counterpart with the rate prescribed by the approximation order of the scheme [12], again, irrespective of what particular $w_n^{(h)}$, $n \in \mathbb{N}^-$, and $g_m^{(h)}$, $m \in \mathbb{M}^-$, are taken on every given grid. As such, one does not need to be overly concerned with the rate of convergence for the discrete optimal control sources as any of those will do the cancellation job equally well anyway.

Let us emphasize that the L_2 optimal solutions for active controls differ very substantially from the L_1 optimal solutions obtained previously in [4]. This is, of course, natural to expect, because minimizing the norms $\|g\|_2$ and $\|g\|_1$ basically means minimizing two quite different (nonlinear) functionals over a vector space.[4] To visualize the corresponding differences, we conduct the L_2 minimization for the same setup, $L = 32$, $J = 7$, and $k = 0.5$, that was earlier analyzed in the sense of L_1, see Fig. 3. The excitation was provided by the point source $f^- = \delta(\mathbf{x} - \mathbf{x}_1)$, where $\mathbf{x}_1 = (5, 0)$. In Fig. 4(a) we show the magnitude of the L_2-optimal active controls on the 32×7 grid. This solution indeed differs drastically from the L_1-optimal controls shown in Fig. 3. Unlike the L_1 optimum, i.e., the layer of surface monopoles, the L_2 optimal solution tends to be distributed over the entire annular region on which the controls are supported, obviously favoring the direction toward the noise source. We have also obtained the L_2 optimal controls

[4] Equivalence of all norms on a finite-dimensional linear space should not lead here to an incorrect assumption that the minima should also be the same, because this equivalence only refers to the convergence with respect to different norms.

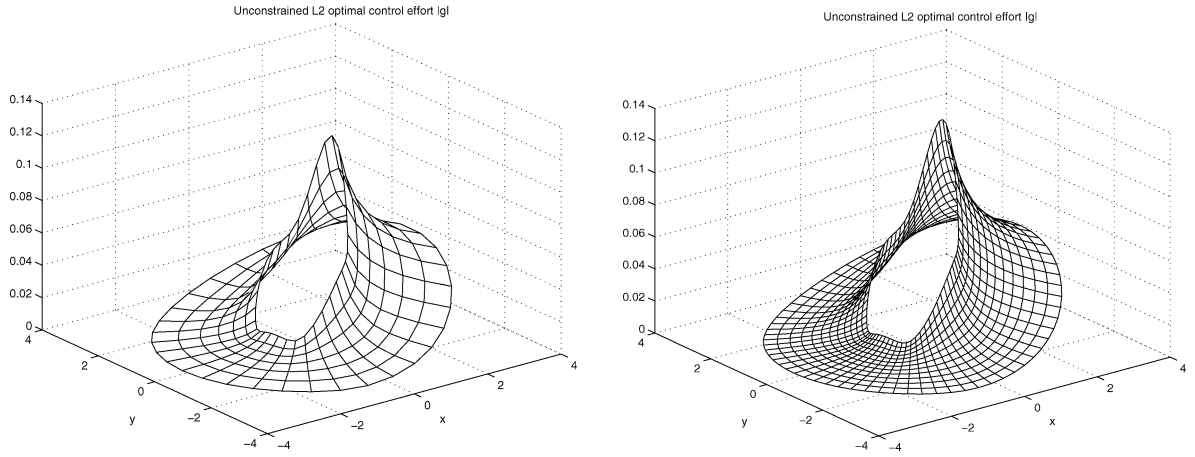

Fig. 4. Magnitude of the L_2-optimal control sources for $\Omega = \{\mathbf{x} \in \mathbb{R}^2 \mid |\mathbf{x}| < 1\}$, $k = 0.5$, $f^- = \delta(\mathbf{x} - \mathbf{x}_1)$, $\mathbf{x}_1 = (5, 0)$: (a) $L = 32$, $J = 7$; (b) $L = 64$, $J = 13$.

for the same case but on the twice as fine grid of dimension 64×13; they are shown in Fig. 4(b). The plots in Fig. 4(a) and (b) look very much alike, as expected.

It is also interesting to observe how the qualitative behavior of the optimal solution changes when the parameters that define the problem vary. A key parameter is the wavenumber k. Previously, we have analyzed the cases of relatively long waves compared to the size (i.e., diameter) of the protected region Ω. Let us now take $k = \pi$, then there will be exactly one full wavelength across the diameter. We compute this case on the grid 128×9 so that $1 = \rho_0 \leqslant \rho \leqslant \rho_{J-1} \approx 1.481$. In Fig. 5, we present the distribution of optimal controls $g^{(h)}$ for the case of the long waves, $k = 0.5$ (Fig. 5(a)), and for the case of the wavelength comparable to the domain size, $k = \pi$ (Fig. 5(b)). The solution that corresponds to shorter waves is clearly more oscillatory.

3.2.2. Constrained optimization in the sense of L_2

The purpose of formulating and solving the L_2 optimization problems that involve constraints was to simulate not simply a more sophisticated geometry but also a more realistic one. For example, if we interpret the previously considered protected region—a unit disk—as a section of the aircraft fuselage, then we can also introduce portholes, i.e., windows, that shall be interpreted as designated areas, in which no control sources can be applied. Optimization problem (27) in this case needs to be modified. Instead of simply finding a weak solution of $\mathbf{Ez} = \mathbf{f}$ in the sense of the least squares, we will now have to impose additional constraints, i.e., require that for those nodes of the grid $\mathbb{M}^-$ that happen to be inside the aforementioned designated areas, the corresponding equations be enforced exactly. This leads to the problem

$$\min_{\mathbf{z}} \|\mathbf{Ez} - \mathbf{f}\|_2 \quad \text{subject to} \quad \mathbf{E}_c\mathbf{z} = \mathbf{f}_c, \tag{32}$$

where $\mathbf{E}_c$ is the sub-matrix of $\mathbf{E}$ (i.e., the appropriate set of rows), and $\mathbf{f}_c$ is the respective sub-vector of $\mathbf{f}$, that correspond to the constrained nodes.

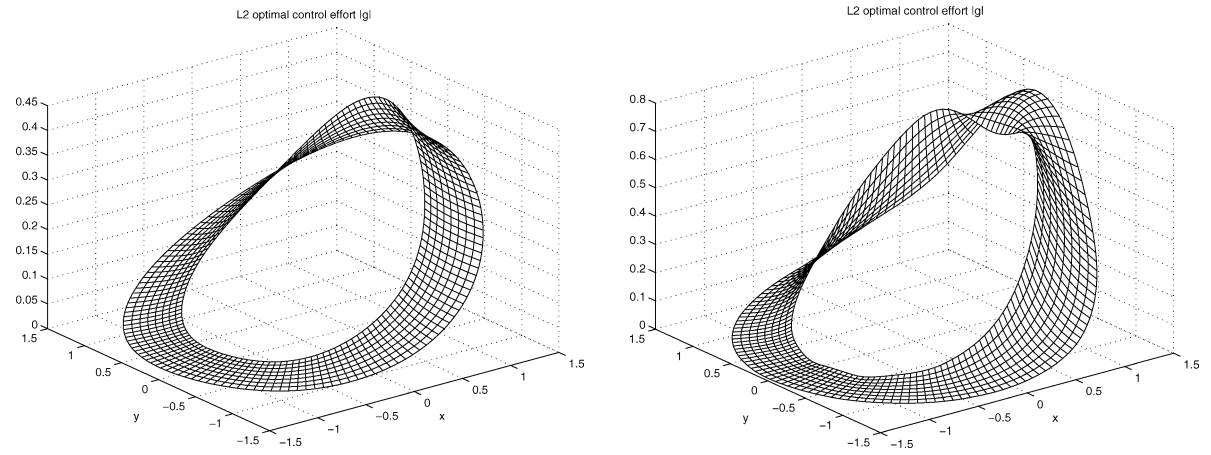

(a) (b)

Fig. 5. Magnitude of the L_2-optimal control sources for $\Omega = \{\mathbf{x} \in \mathbb{R}^2 \mid |\mathbf{x}| < 1\}$, $f^- = \delta(\mathbf{x} - \mathbf{x}_1)$, $\mathbf{x}_1 = (5, 0)$, 128×9 grid: (a) $k = 0.5$; (b) $k = \pi$.

For simulations, we have introduced two symmetrically located portholes in the fuselage: $5^\circ < \theta < 30^\circ$ and $150^\circ < \theta < 175^\circ$. The resulting problem (32) was solved by a standard methodology (procedure `LSQLIN` from MATLAB) that requires linear independence of the constraints.

The case that we have analyzed in the context of the constrained L_2 optimization, was, again, one of those that we have studied previously in the L_1 framework, see [4], but, of course, with no constraints. For this case, the excitation is provided by a pair of external sources: $f^- = \delta(\mathbf{x} - \mathbf{x}_1) + \delta(\mathbf{x} - \mathbf{x}_2)$, where $\mathbf{x}_1 = (5, 0)$ and $\mathbf{x}_2 = (1, 2)$, the wavenumber $k = 0.9$, and the grid has the dimension 48×9. In Fig. 6(a), we show the constrained L_2 optimal solution for this grid, and in Fig. 6(b) we show the solution for the twice as fine grid 96×17. We emphasize the presence of the large spikes in the control effort next to the boundaries of the window on the right, which is natural to expect. We should also point out at some apparent discrepancies between the control field on Fig. 6(a) and that on Fig. 6(b) in the region near this window. Qualitatively, these discrepancies are easily explained once we realize that a given window, which is defined as a particular range of θ, does not have to be exactly the same on different grids because of the finite size $\Delta\theta$, and a finer grid simply provides for a "sharper" definition of the window in the discrete sense. On the other hand, quantitatively we, of course, cannot claim that the same convergence results as we have obtained previously in the case with no constraints, see Section 3.2.1, will hold in the presence of the constraints as well. Moreover, in the constrained case one should generally expect less regularity from the corresponding continuous solution than in the previously addressed unconstrained cases. Therefore, the results of the L_2 constrained minimization should only be regarded as implementation examples of a previously tested numerical algorithm for more elaborate settings.

The actual norms of the solutions that we have obtained are presented in Table 3, which also contains the L_2 norms of surface monopoles optimal in the sense of L_1, see [4]. We see that the L_2 norm at the minimum is considerably larger for the constrained case compared to the unconstrained case. As concerns the L_2 norm of the L_1-optimum, it is three times larger in this case than the unconstrained L_2 minimum. We should also mention that the finer the grid, the larger the L_2 norm of $g^{(\mathrm{h,surf})}_{\mathrm{monopole}}$ is, see Table 3. This is, in fact, a natural consequence of the scaling adopted in [4]. Indeed, the actual magnitude of $g^{(\mathrm{h,surf})}_{\mathrm{monopole}}$ increases when the grid is refined, because the corresponding continuous limit is a single

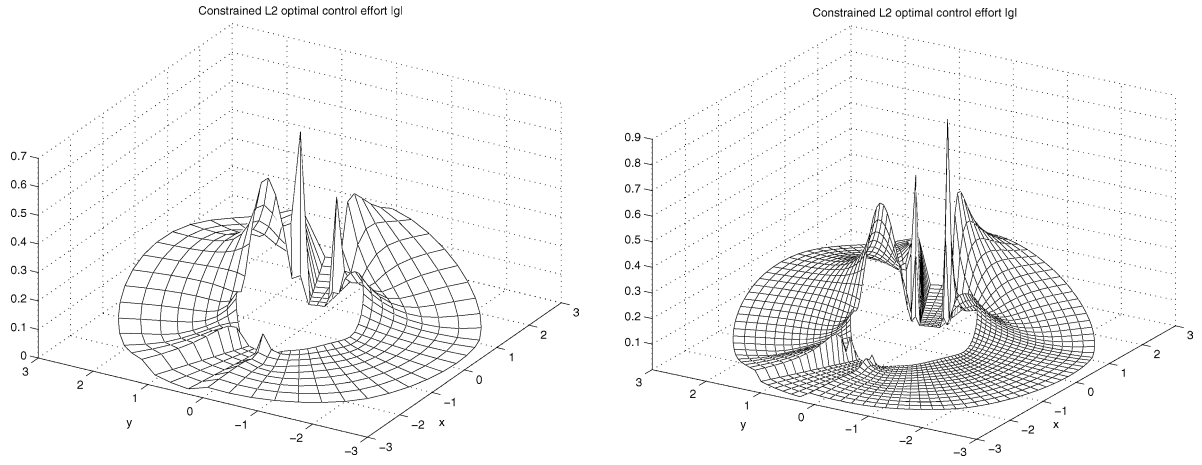

Fig. 6. Magnitude of the L_2-optimal control sources for $\Omega = \{\mathbf{x} \in \mathbb{R}^2 \mid |\mathbf{x}| < 1\}$, $k = 0.9$, excitation: $f^- = \delta(\mathbf{x}-\mathbf{x}_1)+\delta(\mathbf{x}-\mathbf{x}_2)$, $\mathbf{x}_1 = (5, 0)$, $\mathbf{x}_2 = (1, 2)$, and window constraints: $5^\circ < \theta < 30^\circ$ and $150^\circ < \theta < 175^\circ$: (a) $L = 48$, $J = 9$; (b) $L = 96$, $J = 17$.

Table 3
Comparison of the computed L_2-optimal solutions with surface monopoles

Grid	$\min_{w^{(h)}} \|g^{(h)}\|_2^{(h)}$	Constrained $\min_{w^{(h)}} \|g^{(h)}\|_2^{(h)}$	$\|g_{\text{monopole}}^{(\text{h,surf})}\|_2^{(h)}$
48×9	0.41855	0.54013	1.2983
96×17	0.43485	0.56175	1.8315

layer on the interface. The latter is a singular distribution, which is obviously not integrable by itself, and even less so with square. At the same time, it turns out that the discrete two-dimensional L_1 norm of surface monopoles $\|g_{\text{monopole}}^{(\text{h,surf})}\|_{1,\mathbb{M}^-}$ does not change with the change of the grid size. This essentially implies that the magnitude of $g_{\text{monopole}}^{(\text{h,surf})}$ scales as $\mathrm{O}(h^{-1})$ and as such, the L_2 norm $\|g_{\text{monopole}}^{(\text{h,surf})}\|_{2,\mathbb{M}^-}$ is supposed to scale as $\mathrm{O}(h^{-1/2})$. This is corroborated by the data in the last column of Table 3.

4. Discussion

In the paper, we have developed and implemented a computational algorithm for optimizing the sources of active control of sound in the sense of the least squares (L_2). For some simple cases, we have been able to validate our numerical results against spectral solutions. We have also seen that the L_2 optimal controls are distinctly different from the L_1 optimal controls obtained previously. For the case of a somewhat more realistic geometry, the corresponding optimization formulation involves constraints of equality type; this formulation can be analyzed as well. We also emphasize that even though the norm $\|g\|_2$ is hard to characterize using conventional physical terms (for example, it does not correspond to a physical energy like many other L_2 norms do), from the mathematics perspective it still provides a perfectly legitimate quantitative measure of how "big" the control effort $g(\mathbf{x})$ is. As such, minimization of $\|g\|_2$ that we have conducted in this paper is by no means meaningless.

Generally, there is a multitude of optimization criteria that can be used in the context of active control of sound. Unlike $\|g\|_2$, some would admit a clear physical interpretation, such as the control source strength, see [4], or power required by the controls, see [5]. On the other hand, some cost functions, such as $\|g\|_1$ or $\|g\|_2$, would only depend on the controls themselves, whereas others—power-based—would necessarily involve the interaction between the sources of sound and the surrounding acoustic field. As far as different criteria may be concerned, let us note that neither in this paper nor in our previous work on optimization for the active control of sound [4,5] do we favor any specific choice of the function of merit. In particular, neither do we prioritize physical relevance over computational efficacy, nor proceed the other way around. In our opinion, setting priorities of that type is simply not possible while staying within the limits of exact science. What we are rather trying to do is to show that it is very difficult to come up with a universally good optimization criterion, as typically the nice features would come at the expense of one another; that optimal solutions found for different criteria may noticeably differ as well; and that ultimately the choice of the optimization criterion may be determined or at least seriously affected by a number of considerations from "beyond mathematics". Some may originate from the engineering limitations, others will be just a matter of personal preference.

References

[1] S.J. Elliott, Signal Processing for Active Control, Academic Press, San Diego, CA, 2001.
[2] C.R. Fuller, S.J. Elliott, P.A. Nelson, Active Control of Vibration, Academic Press, London, 1996.
[3] L.D. Landau, E.M. Lifshitz, Fluid Mechanics, Pergamon Press, Oxford, 1986.
[4] J. Lončarić, S.V. Tsynkov, Optimization of acoustic source strength in the problems of active noise control, SIAM J. Appl. Math. 63 (4) (2003) 1141–1183.
[5] J. Lončarić, S.V. Tsynkov, Optimization of power in the problems of active control of sound, Math. Comput. Simulation 65 (4–5) (2004) 323–335.
[6] J. Lončarić, V.S. Ryaben'kii, S.V. Tsynkov, Active shielding and control of noise, SIAM J. Appl. Math. 62 (2) (2001) 563–596.
[7] C.L. Morfey, Dictionary of Acoustics, Academic Press, San Diego, CA, 2001.
[8] P.A. Nelson, S.J. Elliott, Active Control of Sound, Academic Press, San Diego, CA, 1999.
[9] Y. Nesterov, A. Nemirovsky, Interior Point Polynomial Methods in Convex Programming: Theory and Algorithms, SIAM, Philadelphia, PA, 1993.
[10] T.W. Roberts, D. Sidilkover, S.V. Tsynkov, On the combined performance of nonlocal artificial boundary conditions with the new generation of advanced multigrid flow solvers, Comput. Fluids 31 (3) (2001) 269–308.
[11] V.S. Ryaben'kii, Necessary and sufficient conditions for good definition of boundary value problems for systems of ordinary difference equations, USSR Comput. Math. Math. Phys. 4 (1964) 43–61.
[12] V.S. Ryaben'kii, Method of Difference Potentials and Its Applications, Springer Series in Computational Mathematics, vol. 30, Springer, Berlin, 2002.
[13] S.V. Tsynkov, Numerical solution of problems on unbounded domains. A review, Appl. Numer. Math. 27 (1998) 465–532.
[14] S.V. Tsynkov, On the definition of surface potentials for finite-difference operators, J. Sci. Comput. 18 (2) (2003) 155–189.
[15] R.J. Vanderbei, Linear Programming: Foundations and Extensions, Kluwer Academic, Boston, 2001.
[16] R.I. Veizman, V.S. Ryaben'kii, Difference problems of screening and simulation, Dokl. Akad. Nauk 354 (1997) 151–154.
[17] R.I. Veizman, V.S. Ryaben'kii, Difference simulation problems, Trans. Moscow Math. Soc. 58 (1997) 239–248.